IET Microwaves, Antennas & Propagation

Research Article

IET Journals
The Institution of Engineering and Technology

Lower bound of the estimation error of an emitter's direction-of-arrival/polarisation, for a collocated triad of orthogonal dipoles/loops that fail randomly

ISSN 1751-8725
Received on 21st October 2016
Accepted on 22nd December 2016
E-First on 24th April 2017
doi: 10.1049/iet-map.2016.0918
www.ietdl.org

Dominic Makaa Kitavi[1], Kainam Thomas Wong[1] ✉, Mengxi Zou[1], Keshav Agrawal[2]

[1]Department of Electronic and Information Engineering, Hong Kong Polytechnic University, Hung Hom, Kowloon, Hong Kong

[2]The Wharton School, University of Pennsylvania, Philadelphia, PA 19104-6340, USA

✉ *E-mail: ktwong@ieee.org*

Abstract: For a triad of short dipoles (or of small loops), in perpendicular orientation relative to each other but collocated in space, this study derives a lower bound for their error in direction-of-arrival estimation and polarisation estimation, accounting for the possibility of failure in any individual dipoles (or loops).

1 Introduction

1.1 Dipole triad and loop triad

A short dipole (a small loop) measures one Cartesian component of an incident electric (magnetic) field vector. With three such dipoles (loops) collocated and oriented orthogonally among themselves, every element of the entire 3×1 electric (magnetic) field vector may be measured distinctly. The collocated orthogonal dipole triad (a.k.a. a 'tripole') has been used in [1–25] for azimuth-elevation direction-finding, tracking, or polarisation estimation. The dipole triad has been implemented in hardware [26] and is commercially available from Winncom Technologies (Solon, OH, USA) for the 5.125–6.1 GHz frequency band.

More precisely, a completely polarised transverse electromagnetic wave with unit power, having travelled through an homogeneous isotropic medium, may be characterised in Cartesian spatial coordinates by its 3×1 electric-field vector [27]:

$$\boldsymbol{e}(\theta,\phi,\gamma,\eta) = \begin{bmatrix} e_x \\ e_y \\ e_z \end{bmatrix} = \begin{bmatrix} \cos(\theta)\cos(\phi) & -\sin(\phi) \\ \cos(\theta)\sin(\phi) & \cos(\phi) \\ -\sin(\theta) & 0 \end{bmatrix} \begin{bmatrix} \sin(\gamma)\mathrm{e}^{\mathrm{j}\eta} \\ \cos(\gamma) \end{bmatrix}, \tag{1}$$

where $\theta \in [0,\pi]$ refers to the polar angle measured from the positive z-axis, $\phi \in [0,2\pi)$ denotes the azimuth angle measured from the positive x-axis, $\gamma \in [0,\pi/2)$ denotes the auxiliary polarisation angle, and $\eta \in [-\pi,\pi)$ is the polarisation phase difference.

The corresponding magnetic field vector equals

$$\boldsymbol{h}(\theta,\phi,\gamma,\eta) = \boldsymbol{e}\left(\theta,\phi,\gamma-\frac{\pi}{2},-\eta\right)\mathrm{e}^{\mathrm{j}\eta}, \tag{2}$$

which represents a duality to the electric-field vector of (1). Hence, the results derived subsequently for a dipole triad are fully applicable to a loop triad, by the changing γ and η as indicated in (2). The collocated orthogonal loop triad has been used in [5, 13, 15, 22, 23, 28] for azimuth-elevation direction-finding, tracking, or polarisation estimation.

1.2 Approximate lower bound that accounts for antenna failure

The Cramér–Rao bound (CRB) lower bounds the variance attainable by any unbiased estimator. For the estimation of the direction-of-arrival/polarisation of a source impinging upon a dipole/loop triad, closed-form expressions of the CRB are derived in [22, 29, 30] explicitly in terms of the signal parameters. The dipole/loop triad's CRB is plotted (but not stated as any closed-form mathematical equation) in [5, 8, 10, 12, 21].

A real-world antenna could fail. To account for such a practical consideration, an approximate lower bound (ALB) is defined in [31] as a weighted sum of various Cramér–Rao bounds, each corresponding to a unique subset of all antennas that are operational.

The summation weights are set equal to the probability of that subset of antennas alone being operational (This ALB has been applied to direction finding at a linear array of L number of uniformly spaced sensors in [31], and at an acoustic vector sensor in [32].).

The present paper will derive this ALB for the direction-of-arrival/polarisation estimation of a dipole/loop triad: (see (3)) and similarly $\mathrm{ALB}_{\geq 2}(\phi)$, $\mathrm{ALB}_{\geq 2}(\gamma)$, and $\mathrm{ALB}_{\geq 2}(\eta)$. In (3), p_x (p_y, p_z) denotes the probability that the x-oriented (y-oriented, z-oriented) antennas could fail. Here, each antenna is assumed to fail independently of all other antennas. If more than one antenna fails in the triad, there would be insufficient data for two-dimensional direction finding or for polarisation estimation.

2 Statistical model of the data

To concentrate on the stochastic breakdown of the antennas, an uncomplicated model of the incident source and the noise will be presumed below. For more complicated source/noise situations, the analytic approach here may be generalised accordingly.

A spatially point-size emitter is fixed in the far field, and emits a unit power sinusoid signal of $s(m) := \sigma_s \exp\{\mathrm{j}((2\pi c/\lambda)Tm + \varphi)\}$ at the mth time instant, with a known amplitude of σ_s, a known

$$\begin{aligned}\mathrm{ALB}_{\geq 2}(\theta) :=\ & (1-p_x)(1-p_y)(1-p_z)\mathrm{CRB}_{x,y,z}(\theta) + p_x(1-p_y)(1-p_z)\mathrm{CRB}_{y,z}(\theta) \\ & +(1-p_x)p_y(1-p_z)\mathrm{CRB}_{x,z}(\theta) + (1-p_x)(1-p_y)p_z\mathrm{CRB}_{x,y}(\theta),\end{aligned} \tag{3}$$

wavelength of λ, a known propagation speed c, a known discrete-time sample period of T, and a known initial phase of φ.

This signal impinges upon a dipole/loop triad located at the spherical coordinates' origin. At this triad, the incident signal is corrupted by an additive noise of $\tilde{\boldsymbol{n}}(m)$, which is modelled as Gaussian distributed, zero in mean, with a diagonal spatial covariance matrix of $\boldsymbol{\Gamma}_0 = \mathrm{diag}[\sigma_n^2, \sigma_n^2, \sigma_n^2]$, and with a white temporal self-correlation.

The scalars θ, ϕ, γ, η, and σ_n are modelled here as deterministic but a priori unknown. They are grouped together to form the elements of a vector $\boldsymbol{\xi} := [\phi, \theta, \gamma, \eta, \sigma_n]$.

At each discrete-time instant m, the triad would collect an $L \times 1$ vector of data:

$$\tilde{z}(m) = \boldsymbol{J}\boldsymbol{e}(\theta, \phi, \gamma, \eta)s(m) + \boldsymbol{J}\tilde{\boldsymbol{n}}(m), \tag{4}$$

where the $L \times 3$ selection matrix $\boldsymbol{J}$ is defined in Table 1.

This selection matrix $\boldsymbol{J}$ arises because the triad's constituent antennas may each either function well or fail, over the entire temporal duration when data are collected. The receiver would disregard any output from any inoperational antenna. Table 1 lists the only seven possible states of the dipole/loop triad. Any two antennas are modelled here as failing with stochastic independence. Direction-finding and polarisation estimation would become infeasible if more than one antenna break down (as in cases #1–#3 in Table 1), but such a scenario would occur very rarely for a well-designed system and is assumed in the subsequent analysis not to occur.

If there exist altogether M number of discrete-time samples, the dataset may be represented as

$$\begin{aligned} \boldsymbol{z} :&= \left[\{\tilde{z}(1)\}^{\mathrm{T}}, \{\tilde{z}(2)\}^{\mathrm{T}}, \ldots, \{\tilde{z}(M)\}^{\mathrm{T}}\right]^{\mathrm{T}} \\ &= \boldsymbol{s} \otimes \boldsymbol{e}(\theta, \phi, \gamma, \eta) + \boldsymbol{n}, \end{aligned} \tag{5}$$

where $\boldsymbol{s} := [s(1), s(2), \ldots, s(M)]^{\mathrm{T}}$, $\boldsymbol{n} := [\{\tilde{\boldsymbol{n}}(1)\}^{\mathrm{T}}, \{\tilde{\boldsymbol{n}}(2)\}^{\mathrm{T}}, \ldots, \{\tilde{\boldsymbol{n}}(M)\}^{\mathrm{T}}]^{\mathrm{T}}$, the superscript T denotes transposition, and $\otimes$ denotes the Kronecker product.

Direction finding aims to estimate the azimuth arrival angle ϕ and the polar arrival angle θ, based on the observation $\boldsymbol{z}$. Polarisation estimation aims to estimate the polarisation parameters of γ and η, also based on the observations $\boldsymbol{z}$.

This paper will derive an ALB for the direction-of-arrival/polarisation estimation error variance, conditioned on the event that the whole receiver system remains operational – in other words, conditional on the event of at least two antennas remain operational. This event corresponds to the union of Table 1's cases #4 to #7.

3 Review of Cramér–Rao bound basics

The CRB lower bounds the variance of the estimation error of any unbiased estimator.

Consider a general case where the azimuth-polar direction-of-arrival (ϕ, θ) and the bivariate polarisation (γ, η) are all deterministically unknown.

Let $\boldsymbol{F}(\boldsymbol{\xi})$ denote the Fisher information matrix (FIM). Its (k, r)th entry equals (see (3.8) on page 72 of [33])

$$[\boldsymbol{F}(\boldsymbol{\xi})]_{k,r} = 2\mathrm{Re}\left\{\left[\frac{\partial \boldsymbol{\mu}}{\partial [\boldsymbol{\xi}]_k}\right]^{\mathrm{H}} \boldsymbol{\Gamma}^{-1} \frac{\partial \boldsymbol{\mu}}{\partial [\boldsymbol{\xi}]_r}\right\} + \mathrm{Tr}\left\{\boldsymbol{\Gamma}^{-1} \frac{\partial \boldsymbol{\Gamma}}{\partial [\boldsymbol{\xi}]_k} \boldsymbol{\Gamma}^{-1} \frac{\partial \boldsymbol{\Gamma}}{\partial [\boldsymbol{\xi}]_r}\right\}, \tag{6}$$

with

$$\boldsymbol{\mu} := E[\boldsymbol{z}] = \boldsymbol{s} \otimes \boldsymbol{J}\boldsymbol{e}(\theta, \phi, \gamma, \eta), \tag{7}$$

$$\boldsymbol{\Gamma} := E\left[(\boldsymbol{z} - \boldsymbol{\mu})(\boldsymbol{z} - \boldsymbol{\mu})^{\mathrm{H}}\right] = \sigma_n^2 \boldsymbol{I}_{LM}, \tag{8}$$

where $\mathrm{Re}\{\cdot\}$ symbolises the real-value part of the entity inside the curly brackets, $\mathrm{Tr}\{\ \}$ denotes the trace of the entity inside the curly brackets, the superscript H indicates conjugate transposition, $E[\ ]$ represents the statistical expectation of the entity inside the square brackets, and $\boldsymbol{I}_{LM}$ refers to an $LM \times LM$ identity matrix.

Since $\boldsymbol{\mu}$ of (8) is independent of σ_n, it holds that $\partial\boldsymbol{\mu}/\partial\sigma_n = \boldsymbol{0}$, thereby rendering the last row and the last column to comprise zero entries only. On the other hand, $\boldsymbol{\Gamma}$ of (8) is independent of θ, ϕ, γ and η, it holds that $\boldsymbol{0} = \partial\boldsymbol{\Gamma}/\partial\theta = \partial\boldsymbol{\Gamma}/\partial\phi = \partial\boldsymbol{\Gamma}/\partial\gamma = \partial\boldsymbol{\Gamma}/\partial\eta$, thereby rendering the trace in (6) to equal zero for all entries of $\boldsymbol{F}(\boldsymbol{\xi})$, except for $[\boldsymbol{F}(\boldsymbol{\xi})]_{5,5}$, which corresponds to only $[\boldsymbol{\xi}]_5 = \sigma_n$. These considerations together give

$$\boldsymbol{F}(\boldsymbol{\xi}) = \begin{bmatrix} F_{\phi,\phi} & F_{\phi,\theta} & F_{\phi,\gamma} & F_{\phi,\eta} & 0 \\ F_{\phi,\theta} & F_{\theta,\theta} & F_{\theta,\gamma} & F_{\theta,\eta} & 0 \\ F_{\phi,\gamma} & F_{\theta,\gamma} & F_{\gamma,\gamma} & F_{\gamma,\eta} & 0 \\ F_{\phi,\eta} & F_{\theta,\eta} & F_{\gamma,\eta} & F_{\eta,\eta} & 0 \\ 0 & 0 & 0 & 0 & F_{\sigma_n,\sigma_n} \end{bmatrix}, \tag{9}$$

where

$$F_{\sigma_n,\sigma_n} = \frac{4LM}{\sigma_n^2}.$$

This block-diagonal form in (9) implies that σ_n is decoupled from the other four unknown parameters. Hence, the last row and the last column of the FIM may henceforth be ignored in the effort to lower bound the estimation of $\phi, \theta, \gamma, \eta$. That is,

Table 1 Various failure cases for the dipole/loop triad (p_ℓ defines the probability of the ℓ-oriented antenna breaking down, with $\ell \in \{x, y, z\}$.)

failure case #	x-axis antenna functional?	y-axis antenna functional?	z-axis antenna functional?	$\boldsymbol{J}$	Probability
1	√	×	×	$[1\ 0\ 0]$	$(1-p_x)p_yp_z$
2	×	√	×	$[0\ 1\ 0]$	$p_x(1-p_y)p_z$
3	×	×	√	$[0\ 0\ 1]$	$p_xp_y(1-p_z)$
4	√	√	×	$\begin{bmatrix}1&0&0\\0&1&0\end{bmatrix}$	$(1-p_x)(1-p_y)p_z$
5	√	×	√	$\begin{bmatrix}1&0&0\\0&0&1\end{bmatrix}$	$(1-p_x)p_y(1-p_z)$
6	×	√	√	$\begin{bmatrix}0&1&0\\0&0&1\end{bmatrix}$	$p_x(1-p_y)(1-p_z)$
7	√	√	√	$\begin{bmatrix}1&0&0\\0&1&0\\0&0&1\end{bmatrix}$	$(1-p_x)(1-p_y)(1-p_z)$

$$\begin{bmatrix} \mathrm{CRB}(\phi) & * & * & * \\ * & \mathrm{CRB}(\theta) & * & * \\ * & * & \mathrm{CRB}(\gamma) & * \\ * & * & * & \mathrm{CRB}(\eta) \end{bmatrix} = \begin{bmatrix} F_{\phi,\phi} & F_{\phi,\theta} & F_{\phi,\gamma} & F_{\phi,\eta} \\ F_{\phi,\theta} & F_{\theta,\theta} & F_{\theta,\gamma} & F_{\theta,\eta} \\ F_{\phi,\gamma} & F_{\theta,\gamma} & F_{\gamma,\gamma} & F_{\gamma,\eta} \\ F_{\phi,\eta} & F_{\theta,\eta} & F_{\gamma,\eta} & F_{\eta,\eta} \end{bmatrix}^{-1}, \tag{10}$$

where * represents elements not of interest to the present investigation.

For the entries remaining in (10):

$$F_{[\boldsymbol{\xi}]_k,[\boldsymbol{\xi}]_r} = \frac{2}{\sigma_n^2}\mathrm{Re}\left\{\left[\frac{\partial \boldsymbol{\mu}}{\partial [\boldsymbol{\xi}]_k}\right]^{\mathrm{H}} \frac{\partial \boldsymbol{\mu}}{\partial [\boldsymbol{\xi}]_r}\right\},$$

where

$$\begin{aligned} \left[\frac{\partial \boldsymbol{\mu}}{\partial [\boldsymbol{\xi}]_k}\right]^{\mathrm{H}} \frac{\partial \boldsymbol{\mu}}{\partial [\boldsymbol{\xi}]_r} &= \left[\boldsymbol{s} \otimes \boldsymbol{J}\frac{\partial \boldsymbol{e}(\theta,\phi,\gamma,\eta)}{\partial [\boldsymbol{\xi}]_k}\right]^{\mathrm{H}} \left[\boldsymbol{s} \otimes \boldsymbol{J}\frac{\partial \boldsymbol{e}(\theta,\phi,\gamma,\eta)}{\partial [\boldsymbol{\xi}]_r}\right] \\ &= \underbrace{\boldsymbol{s}^{\mathrm{H}}\boldsymbol{s}}_{:=\sigma_s^2 M} \otimes \left[\boldsymbol{J}\frac{\partial \boldsymbol{e}(\theta,\phi,\gamma,\eta)}{\partial [\boldsymbol{\xi}]_k}\right]^{\mathrm{H}} \boldsymbol{J}\frac{\partial \boldsymbol{e}(\theta,\phi,\gamma,\eta)}{\partial [\boldsymbol{\xi}]_r} \\ &= M\sigma_s^2 \left[\boldsymbol{J}\frac{\partial \boldsymbol{e}(\theta,\phi,\gamma,\eta)}{\partial [\boldsymbol{\xi}]_k}\right]^{\mathrm{H}} \boldsymbol{J}\frac{\partial \boldsymbol{e}(\theta,\phi,\gamma,\eta)}{\partial [\boldsymbol{\xi}]_r}. \end{aligned}$$

Hence

$$F_{[\boldsymbol{\xi}]_k,[\boldsymbol{\xi}]_r} = 2M\frac{\sigma_s^2}{\sigma_n^2}\mathrm{Re}\left\{\left[\boldsymbol{J}\frac{\partial \boldsymbol{e}(\theta,\phi,\gamma,\eta)}{\partial [\boldsymbol{\xi}]_k}\right]^{\mathrm{H}} \boldsymbol{J}\frac{\partial \boldsymbol{e}(\theta,\phi,\gamma,\eta)}{\partial [\boldsymbol{\xi}]_r}\right\}. \tag{11}$$

The next section will apply (10) and (11) to the various failure cases in Table 1, to derive the 'ALB' of (3).

4 Derivation of the ALB

The following derivation will focus on the dipole triad of (1). The corresponding loop triad results may be obtained via (2).

4.1 If all three antennas operational

When all three antennas are operational, (11) gives

$$\begin{aligned} F_{\phi,\phi} &= 2M\frac{\sigma_s^2}{\sigma_n^2}\mathrm{Re}\left\{\left[\boldsymbol{J}\frac{\partial \boldsymbol{e}(\theta,\phi,\gamma,\eta)}{\partial \phi}\right]^{\mathrm{H}} \boldsymbol{J}\frac{\partial \boldsymbol{e}(\theta,\phi,\gamma,\eta)}{\partial \phi}\right\} \\ &= 2M\frac{\sigma_s^2}{\sigma_n^2}\{1-\sin^2(\theta)\sin^2(\gamma)\}, \\ F_{\phi,\theta} &= 2M\frac{\sigma_s^2}{\sigma_n^2}\mathrm{Re}\left\{\left[\boldsymbol{J}\frac{\partial \boldsymbol{e}(\theta,\phi,\gamma,\eta)}{\partial \phi}\right]^{\mathrm{H}} \boldsymbol{J}\frac{\partial \boldsymbol{e}(\theta,\phi,\gamma,\eta)}{\partial \theta}\right\} \\ &= M\frac{\sigma_s^2}{\sigma_n^2}\sin(\theta)\sin(2\gamma)\cos(\eta), \\ F_{\phi,\gamma} &= 2M\frac{\sigma_s^2}{\sigma_n^2}\mathrm{Re}\left\{\left[\boldsymbol{J}\frac{\partial \boldsymbol{e}(\theta,\phi,\gamma,\eta)}{\partial \phi}\right]^{\mathrm{H}} \boldsymbol{J}\frac{\partial \boldsymbol{e}(\theta,\phi,\gamma,\eta)}{\partial \gamma}\right\} \\ &= -2M\frac{\sigma_s^2}{\sigma_n^2}\cos(\theta)\cos(\eta), \\ F_{\phi,\eta} &= 2M\frac{\sigma_s^2}{\sigma_n^2}\mathrm{Re}\left\{\left[\boldsymbol{J}\frac{\partial \boldsymbol{e}(\theta,\phi,\gamma,\eta)}{\partial \phi}\right]^{\mathrm{H}} \boldsymbol{J}\frac{\partial \boldsymbol{e}(\theta,\phi,\gamma,\eta)}{\partial \eta}\right\} \\ &= M\frac{\sigma_s^2}{\sigma_n^2}\cos(\theta)\sin(2\gamma)\sin(\eta), \\ F_{\theta,\theta} &= 2M\frac{\sigma_s^2}{\sigma_n^2}\mathrm{Re}\left\{\left[\boldsymbol{J}\frac{\partial \boldsymbol{e}(\theta,\phi,\gamma,\eta)}{\partial \theta}\right]^{\mathrm{H}} \boldsymbol{J}\frac{\partial \boldsymbol{e}(\theta,\phi,\gamma,\eta)}{\partial \theta}\right\} \\ &= 2M\frac{\sigma_s^2}{\sigma_n^2}\sin^2(\gamma), \\ F_{\theta,\gamma} &= 2M\frac{\sigma_s^2}{\sigma_n^2}\mathrm{Re}\left\{\left[\boldsymbol{J}\frac{\partial \boldsymbol{e}(\theta,\phi,\gamma,\eta)}{\partial \theta}\right]^{\mathrm{H}} \boldsymbol{J}\frac{\partial \boldsymbol{e}(\theta,\phi,\gamma,\eta)}{\partial \gamma}\right\} \\ &= 0, \\ F_{\theta,\eta} &= 2M\frac{\sigma_s^2}{\sigma_n^2}\mathrm{Re}\left\{\left[\boldsymbol{J}\frac{\partial \boldsymbol{e}(\theta,\phi,\gamma,\eta)}{\partial \theta}\right]^{\mathrm{H}} \boldsymbol{J}\frac{\partial \boldsymbol{e}(\theta,\phi,\gamma,\eta)}{\partial \eta}\right\} \\ &= 0, \\ F_{\gamma,\gamma} &= 2M\frac{\sigma_s^2}{\sigma_n^2}\mathrm{Re}\left\{\left[\boldsymbol{J}\frac{\partial \boldsymbol{e}(\theta,\phi,\gamma,\eta)}{\partial \gamma}\right]^{\mathrm{H}} \boldsymbol{J}\frac{\partial \boldsymbol{e}(\theta,\phi,\gamma,\eta)}{\partial \gamma}\right\} \\ &= 2M\frac{\sigma_s^2}{\sigma_n^2}, \\ F_{\gamma,\eta} &= 2M\frac{\sigma_s^2}{\sigma_n^2}\mathrm{Re}\left\{\left[\boldsymbol{J}\frac{\partial \boldsymbol{e}(\theta,\phi,\gamma,\eta)}{\partial \gamma}\right]^{\mathrm{H}} \boldsymbol{J}\frac{\partial \boldsymbol{e}(\theta,\phi,\gamma,\eta)}{\partial \eta}\right\} \\ &= 0, \\ F_{\eta,\eta} &= 2M\frac{\sigma_s^2}{\sigma_n^2}\mathrm{Re}\left\{\left[\boldsymbol{J}\frac{\partial \boldsymbol{e}(\theta,\phi,\gamma,\eta)}{\partial \eta}\right]^{\mathrm{H}} \boldsymbol{J}\frac{\partial \boldsymbol{e}(\theta,\phi,\gamma,\eta)}{\partial \eta}\right\} \\ &= 2M\frac{\sigma_s^2}{\sigma_n^2}\sin^2(\gamma). \end{aligned}$$

The FIM's 4×4 leading submatrix of (10) becomes

$$M\frac{\sigma_s^2}{\sigma_n^2}\begin{bmatrix} \mathscr{F}_{\phi,\phi} & \mathscr{F}_{\phi,\theta} & \mathscr{F}_{\phi,\gamma} & \mathscr{F}_{\phi,\eta} \\ \mathscr{F}_{\phi,\theta} & 2\sin^2(\gamma) & 0 & 0 \\ \mathscr{F}_{\phi,\gamma} & 0 & 2 & 0 \\ \mathscr{F}_{\phi,\eta} & 0 & 0 & 2\sin^2(\gamma) \end{bmatrix}, \tag{12}$$

with

$$\begin{aligned} \mathscr{F}_{\phi,\phi} &= 2\left\{1-\sin^2(\theta)\sin^2(\gamma)\right\} \\ \mathscr{F}_{\phi,\theta} &= \sin(\theta)\sin(2\gamma)\cos(\eta) \\ \mathscr{F}_{\phi,\gamma} &= -2\cos(\theta)\cos(\eta) \\ \mathscr{F}_{\phi,\eta} &= \cos(\theta)\sin(2\gamma)\sin(\eta). \end{aligned}$$

Using (10), the corresponding Cramér–Rao bounds may be expressed as

$$\begin{aligned} \mathrm{CRB}_{x,y,z}(\phi) &= \left[\{\boldsymbol{F}(\boldsymbol{\xi})\}^{-1}\right]_{1,1} \\ &= \frac{1}{2M}\frac{\sigma_n^2}{\sigma_s^2}\frac{1}{\sin^2(\eta)\{\sin^2(\gamma)+\sin^2(\theta)\cos(2\gamma)\}}, \end{aligned} \tag{13}$$

$$\begin{aligned} \mathrm{CRB}_{x,y,z}(\theta) &= \left[\{\boldsymbol{F}(\boldsymbol{\xi})\}^{-1}\right]_{2,2} \\ &= \frac{1}{2M}\frac{\sigma_n^2}{\sigma_s^2}\frac{\sin^2(\gamma)\sin^2(\eta)\cos^2(\theta)+\cos^2(\gamma)\sin^2(\theta)}{\sin^2(\gamma)\sin^2(\eta)\{\sin^2(\gamma)+\sin^2(\theta)\cos(2\gamma)\}}, \end{aligned} \tag{14}$$

$$\mathrm{CRB}_{x,y,z}(\gamma) = \left[\{\boldsymbol{F}(\boldsymbol{\xi})\}^{-1}\right]_{3,3} = \frac{1}{2M}\frac{\sigma_n^2}{\sigma_s^2}\frac{\cos^2(\theta) - \sin^2(\eta)\cos(2\theta)\cos^2(\gamma)}{\sin^2(\eta)\{\sin^2(\gamma) + \sin^2(\theta)\cos(2\gamma)\}}, \tag{15}$$

$$\mathrm{CRB}_{x,y,z}(\eta) = \left[\{\boldsymbol{F}(\boldsymbol{x})\}^{-1}\right]_{4,4} = \frac{1}{M}\frac{\sigma_n^2}{\sigma_s^2}\frac{1 - \sin^2(\gamma)\sin^2(\theta)}{2\sin^2(\gamma)\{\sin^2(\gamma) + \sin^2(\theta)\cos(2\gamma)\}}. \tag{16}$$

The above subscripts to CRB indicate the axes along which the antennas are operational.

4.2 If only the x-oriented antenna fails

When only the antenna along the x-axis is inoperational, the FIM's 4×4 leading submatrix of (10) becomes

$$M\frac{\sigma_s^2}{\sigma_n^2}\begin{bmatrix} \mathbb{F}_{\phi,\phi} & \mathbb{F}_{\phi,\theta} & \mathbb{F}_{\phi,\gamma} & \mathbb{F}_{\phi,\eta} \\ \mathbb{F}_{\phi,\theta} & \mathbb{F}_{\theta,\theta} & \mathbb{F}_{\theta,\gamma} & \mathbb{F}_{\theta,\eta} \\ \mathbb{F}_{\phi,\gamma} & \mathbb{F}_{\theta,\gamma} & \mathbb{F}_{\gamma,\gamma} & \mathbb{F}_{\gamma,\eta} \\ \mathbb{F}_{\phi,\eta} & \mathbb{F}_{\theta,\eta} & \mathbb{F}_{\gamma,\eta} & \mathbb{F}_{\eta,\eta} \end{bmatrix}, \tag{17}$$

where (see equation below) The corresponding CRB expressions are (see (18) and (19)) (see (19) and (20)) (see (20))

$$\mathrm{CRB}_{y,z}(\eta) = \left[\{\boldsymbol{F}(\boldsymbol{\xi})\}^{-1}\right]_{4,4} = \frac{1}{2M}\frac{\sigma_n^2}{\sigma_s^2}\frac{1}{\sin^2(\gamma)\sin^2(\theta)}. \tag{21}$$

4.3 If only the y-oriented antenna fails

When the antenna along the y-axis is inoperational, the FIM's 4×4 leading submatrix of (10) becomes

$$\begin{aligned}
\mathbb{F}_{\phi,\phi} &= 2\cos^2(\theta)\cos^2(\phi)\sin^2(\gamma) + 2\sin^2(\phi)\cos^2(\gamma) - \cos(\theta)\sin(2\phi)\sin(2\gamma)\cos(\eta), \\
\mathbb{F}_{\phi,\theta} &= \sin(\theta)\sin^2(\phi)\sin(2\gamma)\cos(\eta) - 0.5\sin(2\theta)\sin(2\phi)\sin^2(\gamma), \\
\mathbb{F}_{\phi,\gamma} &= 0.5\{1 + \cos^2(\theta)\}\sin(2\phi)\sin(2\gamma) - 2\cos(\theta)\left\{\sin^2(\phi)\cos(2\gamma) + \sin^2(\gamma)\right\}\cos(\eta), \\
\mathbb{F}_{\phi,\eta} &= \cos(\theta)\sin^2(\phi)\sin(2\gamma)\sin(\eta), \\
\mathbb{F}_{\theta,\theta} &= 2\{1 - \sin^2(\theta)\cos^2(\phi)\}\sin^2(\gamma), \\
\mathbb{F}_{\theta,\gamma} &= 0.5\sin(2\theta)\cos^2(\phi)\sin(2\gamma) + \sin(\theta)\sin(2\phi)\sin^2(\gamma)\cos(\eta), \\
\mathbb{F}_{\theta,\eta} &= 0, \\
\mathbb{F}_{\gamma,\gamma} &= 2\cos^2(\phi)\sin^2(\gamma) + 2\left\{1 - \cos^2(\theta)\cos^2(\phi)\right\}\cos^2(\gamma) - \cos(\theta)\sin(2\phi)\sin(2\gamma)\cos(\eta), \\
\mathbb{F}_{\gamma,\eta} &= \cos(\theta)\sin(2\phi)\sin^2(\gamma)\sin(\eta), \\
\mathbb{F}_{\eta,\eta} &= 2\left\{1 - \cos^2(\theta)\cos^2(\phi)\right\}\sin^2(\gamma).
\end{aligned}$$

$$\mathrm{CRB}_{y,z}(\phi) = \left[\{\boldsymbol{F}(\boldsymbol{\xi})\}^{-1}\right]_{1,1} = \frac{1}{2M}\frac{\sigma_n^2}{\sigma_s^2}\frac{1}{\sin^2(\eta)\sin^2(\theta)} \frac{\begin{array}{c}\cos^2(\gamma)\{\sin^2(\phi) - 0.25\cos^4(\phi)\sin^2(2\theta)\} - \cos^2(\phi)\cos^2(\theta)\{\cos^2(\phi)\cos^2(\theta) - \cos(2\phi)\} \\ +0.25\sin^2(2\phi)\sin^2(\gamma)\{\cos(2\theta)\cos^2(\eta) + 1\} + 0.5\cos(\theta)\sin(2\phi)\sin(2\gamma)\cos(\eta)\{\cos^2(\phi)\cos^2(\theta) - 1\}\end{array}}{\{\sin^2(\gamma)[1 - \sin^2(\theta)\cos^2(\phi)] - \sin^2(\phi)\}^2}, \tag{18}$$

$$\mathrm{CRB}_{y,z}(\theta) = \left[\{\boldsymbol{F}(\boldsymbol{\xi})\}^{-1}\right]_{2,2} = \frac{1}{2M}\frac{\sigma_n^2}{\sigma_s^2}\frac{1}{\sin^2(\gamma)\sin^2(\eta)} \frac{\begin{array}{c}\cos^4(\phi)\cos^2(\theta)\sin^2(\eta) + \cos^2(\gamma)\{\cos^2(\gamma)\sin^2(\phi) + \cos^2(\phi)\cos^2(\theta)[\cos(2\eta) - \cos^2(\phi)\cos^2(\theta)\sin^2(\gamma) \\ -\cos^2(\eta)(1 + \sin^2(\phi))\cos^2(\gamma) + 0.5\sin(2\gamma)\sin(2\phi)\cos(\theta)\cos(\eta)] - 0.5\sin(2\gamma)\sin(2\phi)\cos(\theta)\cos(\eta)\}\end{array}}{\{\sin^2(\gamma)[1 - \sin^2(\theta)\cos^2(\phi)] - \sin^2(\phi)\}^2}, \tag{19}$$

$$\mathrm{CRB}_{y,z}(\gamma) = \left[\{\boldsymbol{F}(\boldsymbol{\xi})\}^{-1}\right]_{3,3} = \frac{1}{2M}\frac{\sigma_n^2}{\sigma_s^2}\frac{1}{\sin^2(\eta)\sin^2(\theta)} \frac{\begin{array}{c}\cos^2(\gamma)\{\sin^2(\theta) + \cos(2\theta)\sin^4(\phi)\cos^2(\eta) + \cos^2(\phi)\cos^2(\theta)[\sin^2(\theta) + \sin^2(\phi)(1 + \sin^2(\theta)) \\ +\cos^2(\phi)\cos^4(\theta)] - [1 + \sin^2(\phi)]\cos^2(\phi)\} + \cos^2(\phi)\cos^4(\theta)\{1 - \cos^2(\phi)\cos^2(\theta)\} \\ +0.5\cos^3(\theta)\sin(2\phi)\sin(2\gamma)\cos(\eta)\{\cos^2(\phi)\cos^2(\theta) - 1\}\end{array}}{\{\sin^2(\gamma)[1 - \sin^2(\theta)\cos^2(\phi)] - \sin^2(\phi)\}^2}, \tag{20}$$

$$M\frac{\sigma_s^2}{\sigma_n^2}\begin{bmatrix}\mathfrak{F}_{\phi,\phi} & \mathfrak{F}_{\phi,\theta} & \mathfrak{F}_{\phi,\gamma} & \mathfrak{F}_{\phi,\eta}\\ \mathfrak{F}_{\phi,\theta} & \mathfrak{F}_{\theta,\theta} & \mathfrak{F}_{\theta,\gamma} & \mathfrak{F}_{\theta,\eta}\\ \mathfrak{F}_{\phi,\gamma} & \mathfrak{F}_{\theta,\gamma} & \mathfrak{F}_{\gamma,\gamma} & \mathfrak{F}_{\gamma,\eta}\\ \mathfrak{F}_{\phi,\eta} & \mathfrak{F}_{\theta,\eta} & \mathfrak{F}_{\gamma,\eta} & \mathfrak{F}_{\eta,\eta}\end{bmatrix}, \tag{22}$$

where (see equation below) The corresponding CRB expressions are (see (23) and (24)) (see (24) and (25)) (see (25))

$$\begin{aligned}\mathrm{CRB}_{x,z}(\eta) &= \left[\{\boldsymbol{F}(\boldsymbol{\xi})\}^{-1}\right]_{4,4}\\ &= \frac{1}{2M}\frac{\sigma_n^2}{\sigma_s^2}\frac{1}{\sin^2(\gamma)\sin^2(\theta)}.\end{aligned} \tag{26}$$

4.4 If only the z-oriented antenna fails

When the antenna along the z-axis is inoperational, the FIM's 4×4 leading submatrix of (10) becomes

$$M\frac{\sigma_s^2}{\sigma_n^2}\begin{bmatrix}\mathcal{F}_{\phi,\phi} & \mathcal{F}_{\phi,\theta} & \mathcal{F}_{\phi,\gamma} & \mathcal{F}_{\phi,\eta}\\ \mathcal{F}_{\phi,\theta} & \mathcal{F}_{\theta,\theta} & \mathcal{F}_{\theta,\gamma} & \mathcal{F}_{\theta,\eta}\\ \mathcal{F}_{\phi,\gamma} & \mathcal{F}_{\theta,\gamma} & \mathcal{F}_{\gamma,\gamma} & \mathcal{F}_{\gamma,\eta}\\ \mathcal{F}_{\phi,\eta} & \mathcal{F}_{\theta,\eta} & \mathcal{F}_{\gamma,\eta} & \mathcal{F}_{\eta,\eta}\end{bmatrix}, \tag{27}$$

where

$$\begin{aligned}
\mathfrak{F}_{\phi,\phi} &= 2\cos^2(\theta)\sin^2(\phi)\sin^2(\gamma) + 2\cos^2(\phi)\cos^2(\gamma) + \cos(\theta)\sin(2\phi)\sin(2\gamma)\cos(\eta),\\
\mathfrak{F}_{\phi,\theta} &= \sin(\theta)\cos^2(\phi)\sin(2\gamma)\cos(\eta) + 0.5\sin(2\theta)\sin(2\phi)\sin^2(\gamma),\\
\mathfrak{F}_{\phi,\gamma} &= 2\cos(\theta)\{\sin^2(\phi)\cos(2\gamma) - \cos^2(\gamma)\}\cos(\eta) - 0.5\{1+\cos^2(\theta)\}\sin(2\phi)\sin(2\gamma),\\
\mathfrak{F}_{\phi,\eta} &= \cos(\theta)\cos^2(\phi)\sin(2\gamma)\sin(\eta),\\
\mathfrak{F}_{\theta,\theta} &= 2\left\{1-\sin^2(\theta)\sin^2(\phi)\right\}\sin^2(\gamma),\\
\mathfrak{F}_{\theta,\gamma} &= 0.5\sin(2\theta)\sin^2(\phi)\sin(2\gamma) - \sin(\theta)\sin(2\phi)\sin^2(\gamma)\cos(\eta),\\
\mathfrak{F}_{\theta,\eta} &= 0,\\
\mathfrak{F}_{\gamma,\gamma} &= 2\sin^2(\phi)\sin^2(\gamma) + 2\cos^2(\gamma)\left\{1-\cos^2(\theta)\sin^2(\phi)\right\} + \cos(\theta)\sin(2\phi)\sin(2\gamma)\cos(\eta),\\
\mathfrak{F}_{\gamma,\eta} &= -\cos(\theta)\sin(2\phi)\sin^2(\gamma)\sin(\eta),\\
\mathfrak{F}_{\eta,\eta} &= 2\left\{1-\cos^2(\theta)\sin^2(\phi)\right\}\sin^2(\gamma).
\end{aligned}$$

$$\begin{aligned}\mathrm{CRB}_{x,z}(\phi) &= \left[\{\boldsymbol{F}(\boldsymbol{\xi})\}^{-1}\right]_{1,1}\\ &= \frac{1}{2M}\frac{\sigma_n^2}{\sigma_s^2}\frac{1}{\sin^2(\theta)\sin^2(\eta)}\\ &\frac{\begin{array}{c}0.25\sin^2(2\phi)\{1+\cos(2\theta)\sin^2(\gamma)\cos^2(\eta)\} + 0.5\cos(\theta)\sin(2\phi)\sin(2\gamma)\cos(\eta)\{1-\sin^2(\phi)\cos^2(\theta)\}\\ +0.25\sin^2(2\theta) + \cos^2(\gamma)\{\cos^4(\phi) - 0.25\sin^4(\phi)\sin^2(2\theta)\}\\ -\cos^2(\phi)\cos^2(\theta)\{\sin^2(\phi) + \sin^2(\theta)[\sin^2(\phi)+1]\}\end{array}}{\{\sin^2(\gamma)[1-\sin^2(\phi)\sin^2(\theta)] - \cos^2(\phi)\}^2},\end{aligned} \tag{23}$$

$$\begin{aligned}\mathrm{CRB}_{x,z}(\theta) &= \left[\{\boldsymbol{F}(\boldsymbol{\xi})\}^{-1}\right]_{2,2}\\ &= \frac{1}{2M}\frac{\sigma_n^2}{\sigma_s^2}\frac{1}{\sin^2(\gamma)\sin^2(\eta)}\\ &\frac{\begin{array}{c}\cos^4(\gamma)\cos^2(\theta)\cos^2(\eta)\{\cos^4(\phi)-1\}\\ +\sin^4(\phi)\cos^2(\theta)\sin^2(\eta) + 0.5\cos(\theta)\sin(2\phi)\cos^2(\gamma)\sin(2\gamma)\cos(\eta)\{1-\cos^2(\theta)\sin^2(\phi)\}\\ +\cos^4(\gamma)\{\cos^2(\phi) + \cos^4(\theta)\sin^4(\phi)\} + \cos^2(\gamma)\cos^2(\theta)\sin^2(\phi)\{\cos(2\eta) - \cos^2(\theta)\sin^2(\phi)\}\end{array}}{\{\sin^2(\gamma)[1-\sin^2(\phi)\sin^2(\theta)] - \cos^2(\phi)\}^2},\end{aligned} \tag{24}$$

$$\begin{aligned}\mathrm{CRB}_{x,z}(\gamma) &= \left[\{\boldsymbol{F}(\boldsymbol{\xi})\}^{-1}\right]_{3,3}\\ &= \frac{1}{2M}\frac{\sigma_n^2}{\sigma_s^2}\frac{1}{\sin^2(\theta)\sin^2(\eta)}\\ &\frac{\begin{array}{c}\cos^2(\gamma)\{\cos^4(\phi) - \cos^4(\theta)\sin^2(\theta) + \cos^2(\phi)\cos^2(\theta)[\sin^2(\phi) - \sin^2(\theta)\cos^2(\phi) - (1+\sin^2(\phi))\cos^4(\theta)]\}\\ +\cos(2\theta)\cos^4(\phi)\cos^2(\gamma)\cos^2(\eta) + 0.5\cos^3(\theta)\sin(2\phi)\sin(2\gamma)\cos(\eta)\{1-\sin^2(\phi)\cos^2(\theta)\}\\ +\cos^4(\theta)\sin^2(\phi)\{1-\cos^2(\theta)\sin^2(\phi)\}\end{array}}{\{\sin^2(\gamma)[1-\sin^2(\phi)\sin^2(\theta)] - \cos^2(\phi)\}^2},\end{aligned} \tag{25}$$

$$\mathcal{F}_{\phi,\phi} = 2\{1-\sin^2(\theta)\sin^2(\gamma)\},$$
$$\mathcal{F}_{\phi,\theta} = \sin(\theta)\sin(2\gamma)\cos(\eta),$$
$$\mathcal{F}_{\phi,\gamma} = -2\cos(\theta)\cos(\eta),$$
$$\mathcal{F}_{\phi,\eta} = \cos(\theta)\sin(2\gamma)\sin(\eta),$$
$$\mathcal{F}_{\theta,\theta} = 2\sin^2(\theta)\sin^2(\gamma),$$
$$\mathcal{F}_{\theta,\gamma} = -0.5\sin(2\theta)\sin(2\gamma),$$
$$\mathcal{F}_{\theta,\eta} = 0,$$
$$\mathcal{F}_{\gamma,\gamma} = 2\{1-\sin^2(\theta)\cos^2(\gamma),\}$$
$$\mathcal{F}_{\gamma,\eta} = 0,$$
$$\mathcal{F}_{\eta,\eta} = 2\cos^2(\theta)\sin^2(\gamma).$$

The corresponding CRB expressions are

$$\mathrm{CRB}_{x,y}(\phi) = \left[\{\boldsymbol{F}(\boldsymbol{\xi})\}^{-1}\right]_{1,1} = \frac{1}{2M}\frac{\sigma_n^2}{\sigma_s^2}\frac{1}{\cos^2(\theta)\sin^2(\gamma)\sin^2(\eta)}, \tag{28}$$

(see (29))

$$\mathrm{CRB}_{x,y}(\gamma) = \left[\{\boldsymbol{F}(\boldsymbol{\xi})\}^{-1}\right]_{3,3} = \frac{1}{2M}\frac{\sigma_n^2}{\sigma_s^2}\frac{1}{\sin^2(\gamma)\sin^2(\eta)}, \tag{30}$$

$$\mathrm{CRB}_{x,y}(\eta) = \left[\{\boldsymbol{F}(\boldsymbol{\xi})\}^{-1}\right]_{4,4} = \frac{1}{2M}\frac{\sigma_n^2}{\sigma_s^2}\frac{1-\sin^2(\gamma)\sin^2(\theta)}{\cos^4(\theta)\sin^4(\gamma)}. \tag{31}$$

4.5 Approximate lower bound

If the triad has more than one of its constituent-antennas failing, there would be insufficient data to estimate $(\phi,\theta,\gamma,\eta)$. For example, if two constituent-antennas fail, there would only be one complex-value scalar time series of observation, but four real-value parameters in $(\phi,\theta,\gamma,\eta)$ to be estimated.

Hence, conditioned on at least two constituent antennas being operational, the ALB equals (see (32)) where $(\cdot)$ refers to any of (ϕ), (θ), (γ), and (η). The above numerator's four terms correspond to cases #4–#7 of Table 1.

$\mathrm{ALB}_{\geq 2}(\cdot) \to \mathrm{CRB}_{x,y,z}(\cdot)$ as $p_f \to 0$ which is expected since when the probability of any antenna failure is zero, then the problem will reduce to the only case where all antennas are functional.

Fig. 1 shows the four 'approximate lower bounds' $\left(\text{i.e. } \mathrm{ALB}_{\geq 2}(\theta), \mathrm{ALB}_{\geq 2}(\phi), \mathrm{ALB}_{\geq 2}(\gamma), \mathrm{ALB}_{\geq 2}(\eta)\right)$ at various values of the failure rate (p_f) and at various polarisation states. There, the impinging signal has its polarisation phase difference (η) varying from 90° to 0° to −90°, with the auxiliary polarisation angle (γ) constant at 45° – i.e. from left circular polarisation, to 45° linear polarisation, to right circular polarisation. The other parameters are set at $\theta = 40^\circ$, $\phi = 30^\circ$, $M = 200$ snapshots, and signal-to-noise power ratios (SNR): $\sigma_s^2/\sigma_n^2 = 20$ dB. Fig. 1 shows benchmarks to the engineer in his/her tripole design to meet a given level of estimation error. In that figure, all four $\mathrm{ALB}_{\geq 2}(\cdot)$ clearly increases with an increasing p_f, but not linearly so ($\mathrm{ALB}_{\geq 2}(\phi)$, $\mathrm{ALB}_{\geq 2}(\theta)$, and $\mathrm{ALB}_{\geq 2}(\gamma) \to \infty$, as $\eta \to 0$. This is because of the $\sin\eta$ factor in the denominators of the various CRBs in Sections 4.1–4.4. This is not caused by $p_\mathrm{f} \neq 0$, but is an inherent limitation of the tripole as a sensing system.).

5 Special case of Section 4, now with the incident signal being left-hand circular polarisation ($\eta = \pi/2, \gamma = \pi/4$)

The preceding Section 4 has derived the ALB for an incident signal of any azimuth-polar direction-of-arrival (ϕ,θ) and any polarisation (γ,η). To visualise how each antenna's failure probability p_f may affect the ALB, this section will consider the special case of the incident signal being left-hand circularly polarised, i.e. $\eta = \pi/2$ and $\gamma = \pi/4$.

5.1 All three antennas operational

Substituting $\eta = \pi/2$ and $\gamma = \pi/4$ into (13)–(16),

$$\mathrm{CRB}_{x,y,z}(\phi) = \frac{1}{M}\frac{\sigma_n^2}{\sigma_s^2}, \tag{33}$$

$$\mathrm{CRB}_{x,y,z}(\theta) = \frac{1}{M}\frac{\sigma_n^2}{\sigma_s^2}, \tag{34}$$

$$\mathrm{CRB}_{x,y,z}(\gamma) = \frac{1}{2M}\frac{\sigma_n^2}{\sigma_s^2}, \tag{35}$$

$$\mathrm{CRB}_{x,y,z}(\eta) = \frac{1}{M}\frac{\sigma_n^2}{\sigma_s^2}\{1+\cos^2(\theta)\}. \tag{36}$$

For any finite $(1/2M)(\sigma_n^2/\sigma_s^2)$, each CRB above must be finite.

5.2 Only antenna along x-axis inoperational

Substituting $\eta = \pi/2$ and $\gamma = \pi/4$ into (18)–(21),

$$\mathrm{CRB}_{y,z}(\phi) = \frac{1}{M}\frac{\sigma_n^2}{\sigma_s^2}\frac{\cos^2(\theta)\{\sin^2(\theta)+\sin^4(\phi)\}+\sin^2(\phi)\sin^4(\theta)\{1+\cos^2(\phi)\}}{\sin^2(\theta)\{\sin^2(\theta)\cos^2(\phi)-\cos(2\phi)\}^2}, \tag{37}$$

$$\mathrm{CRB}_{x,y}(\theta) = \left[\{\boldsymbol{F}(\boldsymbol{\xi})\}^{-1}\right]_{2,2} = \frac{2}{M}\frac{\sigma_n^2}{\sigma_s^2}\frac{\sin^2(\eta)\{\cos(2\theta)+\sin^2(\gamma)\sin^2(\theta)\}+\cos^2(\gamma)\sin^4(\theta)}{\sin^2(2\theta)\sin^4(\gamma)\sin^2(\eta)}, \tag{29}$$

$$\mathrm{ALB}_{\geq 2}(\cdot) = \frac{p_\mathrm{f}(1-p_\mathrm{f})^2\left\{\mathrm{CRB}_{x,y}(\cdot)+\mathrm{CRB}_{x,z}(\cdot)+\mathrm{CRB}_{y,z}(\cdot)\right\}+(1-p_\mathrm{f})^3\mathrm{CRB}_{x,y,z}(\cdot)}{\underbrace{\sum_{L=2}^{3}\binom{3}{L}(1-p_\mathrm{f})^L p_\mathrm{f}^{3-L}}_{=(1+2p_\mathrm{f})(1-p_\mathrm{f})^2}} = \frac{p_\mathrm{f}\left\{\mathrm{CRB}_{x,y}(\cdot)+\mathrm{CRB}_{x,z}(\cdot)+\mathrm{CRB}_{y,z}(\cdot)\right\}+(1-p_f)\mathrm{CRB}_{x,y,z}(\cdot)}{1+2p_\mathrm{f}}, \tag{32}$$

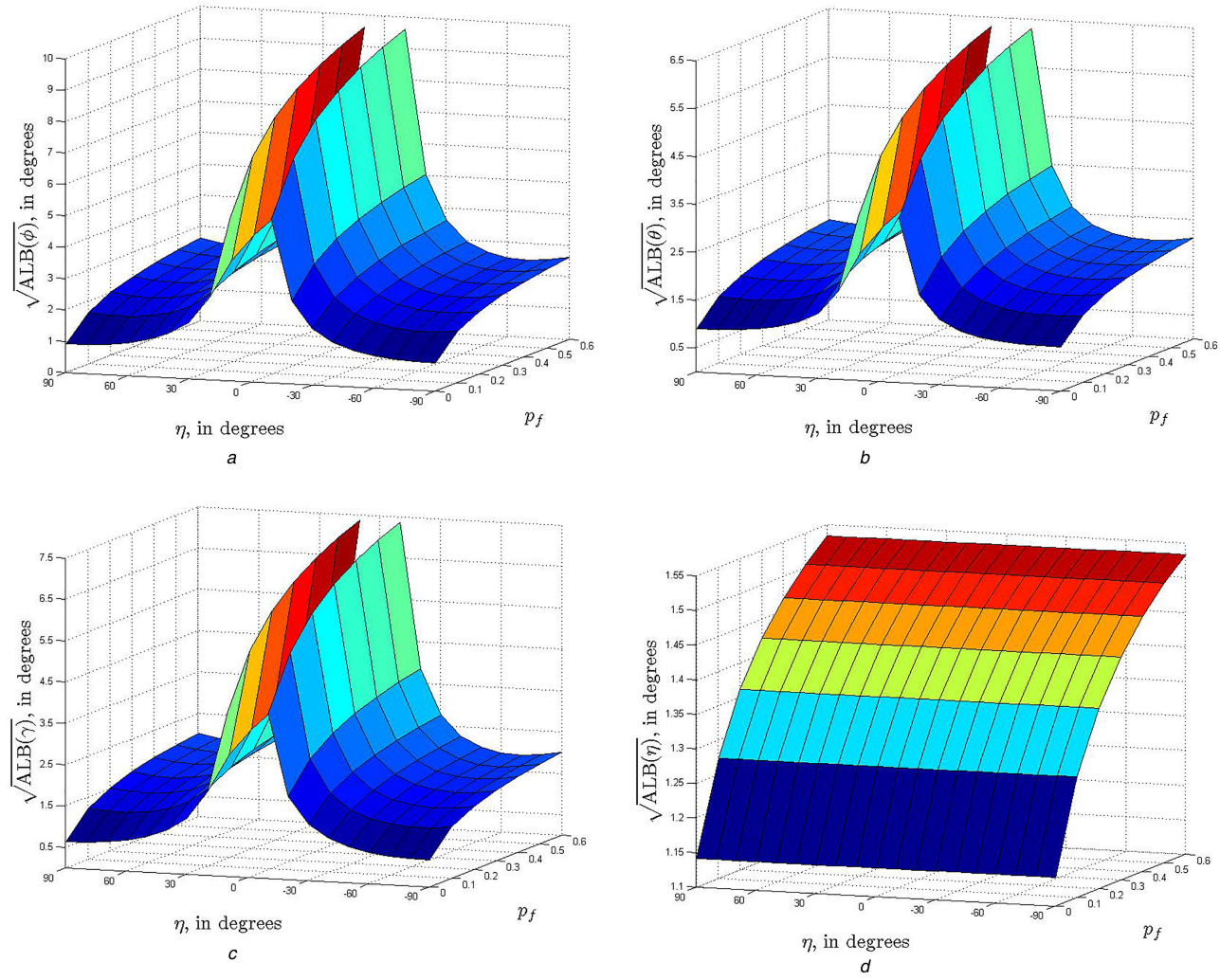

Fig. 1

(a) $\text{ALB}_{\geq 2}(\phi)$, ***(b)*** $\text{ALB}_{\geq 2}(\theta)$, ***(c)*** $\text{ALB}_{\geq 2}(\gamma)$, ***(d)*** $\text{ALB}_{\geq 2}(\eta)$ – each versus the incident signal's polarisations and versus the dipoles' failure rate

$$\text{CRB}_{y,z}(\theta) = \frac{1}{M}\frac{\sigma_n^2}{\sigma_s^2}\frac{1-\sin^4(\theta)\cos^4(\phi)-0.25\sin^2(2\phi)\{1+2\cos^2(\theta)\}}{\{\sin^2(\theta)\cos^2(\phi)-\cos(2\phi)\}^2}, \tag{38}$$

$$\text{CRB}_{y,z}(\gamma) = \frac{1}{M}\frac{\sigma_n^2}{\sigma_s^2}\frac{0.25\cos^2(\theta)\cos(2\theta)\sin^2(2\phi)+\sin^2(\theta)\{1-\sin^2(\theta)\cos^2(\phi)\}^2}{\sin^2(\theta)\{\sin^2(\theta)\cos^2(\phi)-\cos(2\phi)\}^2}, \tag{39}$$

$$\text{CRB}_{y,z}(\eta) = \frac{1}{M}\frac{\sigma_n^2}{\sigma_s^2}\frac{1}{\sin^2(\theta)}. \tag{40}$$

The multiplicative factor $\sin(\theta)$ appears in the denominators of $\text{CRB}_{y,z}(\phi)$, $\text{CRB}_{y,z}(\gamma)$, and $\text{CRB}_{y,z}(\eta)$ – all of which would approach ∞ as $\theta \to 0, \pi$.

Moreover, the multiplicative factor $\sin^2(\theta)\cos^2(\phi)-\cos(2\phi)$ appears in the denominators of $\text{CRB}_{y,z}(\phi)$, $\text{CRB}_{y,z}(\theta)$, and $\text{CRB}_{y,z}(\gamma)$ – all of which would approach ∞ as $\sin^2(\theta)\cos^2(\phi)-\cos(2\phi) \to 0$.

5.3 Only antenna along y-axis inoperational

Substituting $\eta = \pi/2$ and $\gamma = \pi/4$ into (23)–(26),

$$\text{CRB}_{x,z}(\phi) = \frac{1}{M}\frac{\sigma_n^2}{\sigma_s^2}\frac{1-\sin^2(\phi)\{[1+\cos^2(\phi)]\cos^2(\theta)+\sin^2(\phi)\sin^4(\theta)\}}{\sin^2(\theta)\{\sin^2(\theta)\sin^2(\phi)+\cos(2\phi)\}^2}, \tag{41}$$

$$\text{CRB}_{x,z}(\theta) = \frac{1}{M}\frac{\sigma_n^2}{\sigma_s^2}\frac{1-\sin^2(\phi)\{\sin^2(\theta)[\sin^2(\theta)\sin^2(\phi)-2\cos^2(\phi)]+3\cos^2(\phi)\}}{\{\sin^2(\theta)\sin^2(\phi)+\cos(2\phi)\}^2}, \tag{42}$$

(see (43))

$$\text{CRB}_{x,z}(\eta) = \frac{1}{M}\frac{\sigma_n^2}{\sigma_s^2}\frac{1}{\sin^2(\theta)}. \tag{44}$$

As in Section 5.2, the multiplicative factor $\sin(\theta)$ appears here in the denominators of $\text{CRB}_{y,z}(\phi)$, $\text{CRB}_{y,z}(\gamma)$, and $\text{CRB}_{y,z}(\eta)$ – all of which would approach ∞ as $\theta \to 0, \pi$.

$$\text{CRB}_{x,z}(\gamma) = \frac{1}{M}\frac{\sigma_n^2}{\sigma_s^2}\frac{0.25\sin^2(2\phi)\{1-3\sin^2(\theta)\}+\sin^2(\theta)-\sin^4(\theta)\sin^4(\phi)\{1+\cos^2(\theta)\}}{\sin^2(\theta)\{\sin^2(\theta)\sin^2(\phi)+\cos(2\phi)\}^2}, \tag{43}$$

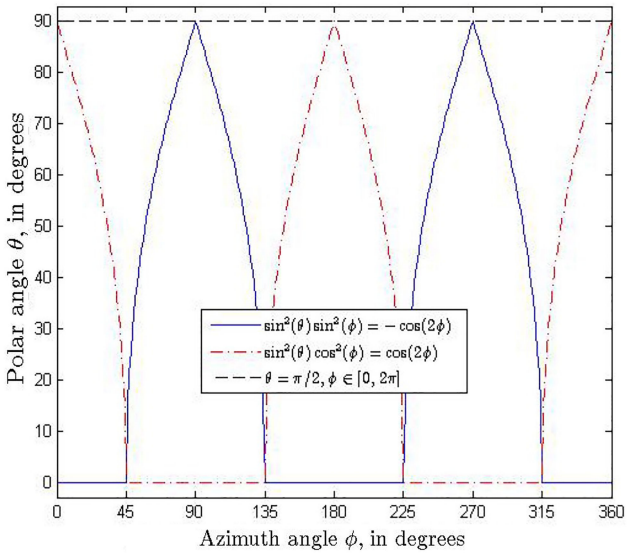

Fig. 2 *Regions (contours) where* $ALB_{\geq 2}(\phi)$ *would be infinite*

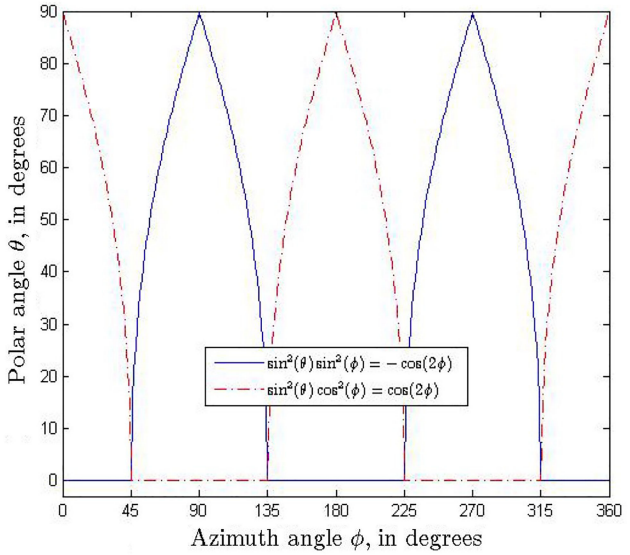

Fig. 3 *Regions (contours) where* $ALB_{\geq 2}(\theta)$ *would be infinite (also applicable to* $\mathrm{ALB}_{\geq 2}(\gamma)$*)*

Moreover, the multiplicative factor $\sin^2(\theta)\sin^2(\phi) + \cos(2\phi)$ appears in the denominators of $\mathrm{CRB}_{y,z}(\phi)$, $\mathrm{CRB}_{y,z}(\theta)$, and $\mathrm{CRB}_{y,z}(\gamma)$ – all of which would approach ∞ as $\sin^2(\theta)\sin^2(\phi) + \cos(2\phi) \to 0$.

5.4 Only antenna along z-axis inoperational

Substituting $\eta = \pi/2$ and $\gamma = \pi/4$ into (28)–(31),

$$\mathrm{CRB}_{x,y}(\phi) = \frac{1}{M}\frac{\sigma_n^2}{\sigma_s^2}\frac{1}{\cos^2(\theta)}, \tag{45}$$

$$\mathrm{CRB}_{x,y}(\theta) = \frac{1}{M}\frac{\sigma_n^2}{\sigma_s^2}\frac{1+\cos^2(\theta)}{\sin^2(\theta)}, \tag{46}$$

$$\mathrm{CRB}_{x,y}(\gamma) = \frac{1}{M}\frac{\sigma_n^2}{\sigma_s^2}, \tag{47}$$

$$\mathrm{CRB}_{x,y}(\eta) = \frac{1}{M}\frac{\sigma_n^2}{\sigma_s^2}\frac{1+\cos^2(\theta)}{\cos^4(\theta)}. \tag{48}$$

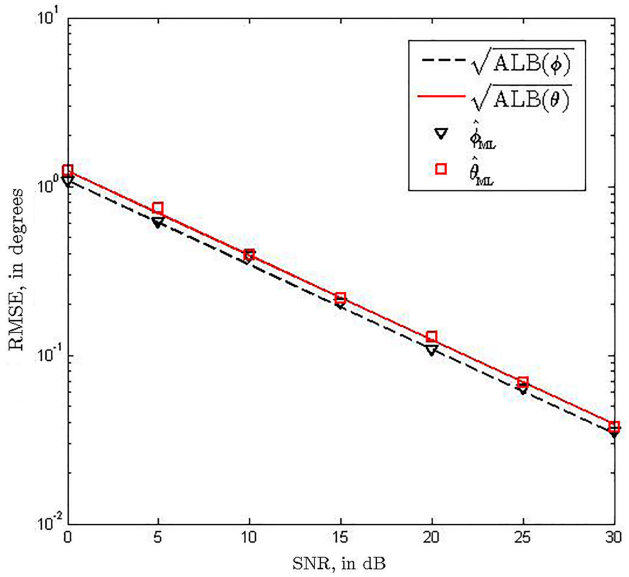

Fig. 4 *Tightness of the proposed/derived* $ALB_{\geq 2}(\theta)$ *and* $ALB_{\geq 2}(\phi)$ *at various SNR*

As in Section 5.2, the multiplicative factor $\sin(\theta)$ appears here in the denominators of $\mathrm{CRB}_{y,z}(\theta)$, which would approach ∞ as $\theta \to 0, \pi$.

Furthermore, the multiplicative factor $\cos(\theta)$ appears in the denominators of $\mathrm{CRB}_{y,z}(\phi)$ and $\mathrm{CRB}_{y,z}(\eta)$ – both of which would approach ∞ as $\theta \to \pi/2$.

5.5 Approximate lower bound

From the ALB expression of (32), the ALB $(\cdot)$ would approach infinity if any of $\mathrm{CRB}_{x,y}(\cdot)$, $\mathrm{CRB}_{x,z}(\cdot)$, $\mathrm{CRB}_{y,z}(\cdot)$, and $\mathrm{CRB}_{x,y,z}(\cdot)$ approaches infinity.

This implies, for any non-zero p_{f}, that

A. $\mathrm{ALB}_{\geq 2}(\phi) \to \infty$ if

i. $\theta = \pi/2$, or
ii. $\sin^2(\theta)\sin^2(\phi) = -\cos(2\phi)$, or
iii. $\sin^2(\theta)\cos^2(\phi) = \cos(2\phi)$.

These contours are plotted in Fig. 2.

B. $\mathrm{ALB}_{\geq 2}(\theta) \to \infty$ if

i. $\sin^2(\theta)\sin^2(\phi) = -\cos(2\phi)$, or
ii. $\sin^2(\theta)\cos^2(\phi) = \cos(2\phi)$.

These contours are plotted in Fig. 3.

C. $\mathrm{ALB}_{\geq 2}(\gamma) \to \infty$ if

i. $\sin^2(\theta)\sin^2(\phi) = -\cos(2\phi)$, or
ii. $\sin^2(\theta)\cos^2(\phi) = \cos(2\phi)$.

These contours are plotted in Fig. 3.

D. $\mathrm{ALB}_{\geq 2}(\eta) \to \infty$, if $\theta \in \{0, \pi/2, \pi\}$.

6 Monte Carlo simulations

To illustrate the tightness of the approximate lower bounds of (32) that family of bounds are compared here against the maximum-likelihood estimate, through Monte Carlo simulations. The simulation settings are as follows: $\theta = 43^\circ$, $\phi = 39^\circ$, $\gamma = 37^\circ$, $\eta = 63^\circ$, $\varphi = 41^\circ$, $p_{\mathrm{f}} = 0.1$, and $(c/\lambda)T = 0.3$, $M = 100$ time

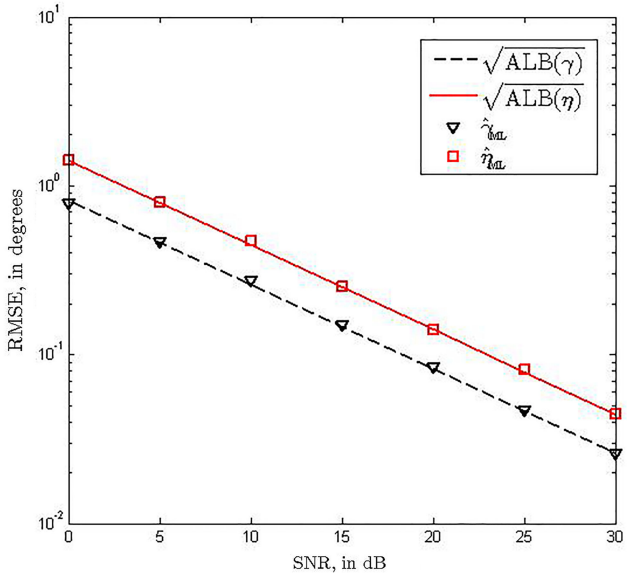

Fig. 5 *Tightness of the proposed/derived* $ALB_{\geq 2}(\gamma)$ *and* $ALB_{\geq 2}(\eta)$ *at various SNR*

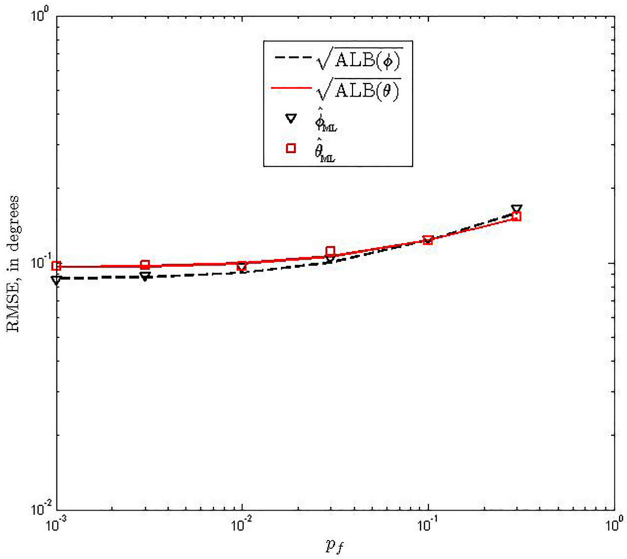

Fig. 6 *Tightness of the proposed/derived* $ALB_{\geq 2}(\theta)$ *and* $ALB_{\geq 2}(\phi)$ *at various failure rates* (p_f)

samples, and $P = 1000$ independent Monte Carlo experiments per icon in each graph. Figs. 4 and 5 show that the ALB of (32) tightly predicts the Monte Carlo simulations' root-mean-square error of the direction-of-arrival and polarisation at various SNR ($\mathrm{RMSE}(\hat{\theta}) := \sqrt{(1/P)\sum_{p=1}^{P}\left(\hat{\phi}_p - \phi\right)^2}$ for the azimuth angle, where $\hat{\theta}_p$ represents the estimate in the pth Monte Carlo experiment. Similarly, $\mathrm{RMSE}(\hat{\phi})$, $\mathrm{RMSE}(\hat{\gamma})$, and $\mathrm{RMSE}(\hat{\eta})$ may be defined.). Figs. 6 and 7 show a similar tightness over various failure rates (p_f). There, the SNR equals 10 dB.

7 Conclusion

This work proposes a lower bound for the estimation of an incident electromagnetic signal's direction-of-arrival and polarisation, using a triad of collocated and perpendicular dipoles that are electrically short. This lower bound's singularity region is the union of its constituent Cramér–Rao bounds' singularity regions. These new lower bounds are expressed analytically and plotted graphically in terms of individual dipoles' failure rate. These provide benchmarks to the engineer in his/her tripole design to meet a given level of estimation error.

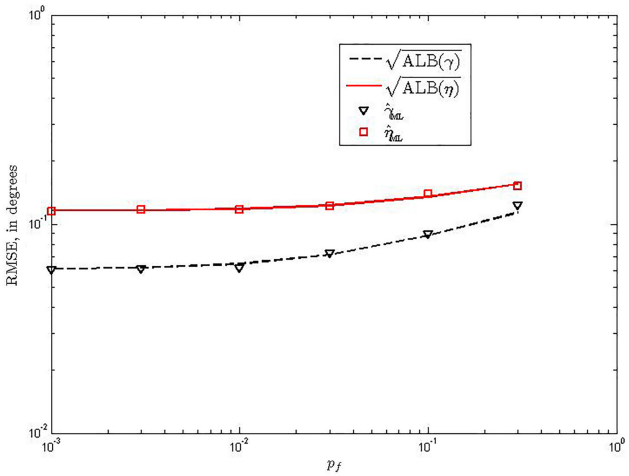

Fig. 7 *Tightness of the proposed/derived* $ALB_{\geq 2}(\gamma)$ *and* $ALB_{\geq 2}(\eta)$ *at various failure rates* (p_f)

While this paper examines only the admittedly simple case of one incident source at one tripole, the approach here may be readily extended to the case of many source impinging upon many tripoles. Though the preceding analysis has focused on the dipole triad of (1), a corresponding analysis for a loop triad may readily be obtained via (2).

8 References

[1] Lecacheux, A.: 'Direction finding of a radiosource of unknown polarization with short electric antennas on a spacecraft', *Astron. Astrophys.*, 1978, **70**, pp. 701–706

[2] Ratnarajah, T.: 'An H^{∞} approach to multi-source tracking'. IEEE Int. Conf. on Acoustics, Speech and Signal Processing, 1998, vol. **4**, pp. 2205–2208

[3] Afraimovich, E.L., Chernukhov, V.V., Kobzar, V.A., *et al.*: 'Determining polarization parameters & angles of arrival of HF radio signals using three mutually orthogonal antennas', *Radio Sci.*, 1999, **34**, (5), pp. 1217–1225

[4] Roussy, G., Agbossou, K., Dichtel, B.: 'Vector electric field measurement using a non-interfering sensor', *Meas. Sci. Technol.*, 2000, **11**, pp. 1145–1151

[5] Wong, K.T.: 'Direction finding/polarization estimation – dipole and/or Loop triad(s)', *IEEE Trans. Aerosp. Electron. Syst.*, 2001, **37**, (2), pp. 679–684

[6] Panchenko, M.: 'Direction finding of AKR sources with three orthogonal antennas', 2003, **38**, (6)

[7] Lundback, J., Nordebo, S.: 'On polarization estimation using tripole arrays'. IEEE Antennas-Propagation Society Int. Symp., 2003, vol. **1**, pp. 65–68

[8] Lundback, J., Nordebo, S.: 'Analysis of a tripole array for polarization & direction of arrival estimation'. IEEE Sensor Array and Multichannel Signal Processing Workshop, 2004, pp. 284–288

[9] Cecconi, B., Zarka, P.: 'Direction finding and antenna calibration through analytical inversion of radio measurements performed using a system of two or three electric dipole antennas on a three-axis stabilized spacecraft', *Radio Sci.*, 2005, **40**, (3), pp. 1–20

[10] Nordebo, S., Gustafsson, M., Lundback, J.: 'Fundamental limitations for DOA and polarization estimation with applications in array signal processing', *IEEE Trans. Signal Process.*, 2006, **54**, (10), pp. 4055–4061

[11] Xu, Y., Liu, Z.: 'Adaptive quasi-cross-product algorithm for uni-tripole tracking of moving source'. Int. Conf. on Communication Technology, 2006

[12] Zhang, X., Shi, Y., Xu, D.: 'Novel blind joint direction of arrival and polarization estimation for polarization-sensitive uniform circular array', *Prog. Electromagn. Res.*, 2008, **86**, pp. 19–37

[13] Xu, Y., Liu, Z., Fu, S.: 'Polarimetric smoothing revisited: applicability to randomly polarized sources and to incomplete electromagnetic vector-sensors'. Int. Conf. on Signal Processing, 2008, pp. 328–331

[14] Zainud-Deen, S.H., Malhat, H.A., Awadalla, K.H., *et al.*: 'Direction of arrival and state of polarization estimation using radial basis function neural network (RBFNN)'. National Radio Science Conf., 2008

[15] Gong, X., Liu, Z., Xu, Y., *et al.*: 'Direction-of-arrival estimation via twofold mode-projection', *Signal Process.*, 2009, **89**, pp. 831–842

[16] Daldorff, L.K.S., Turaga, D.S., Verscheure, O., *et al.*: 'Direction of arrival estimation using single tripole radio antenna'. IEEE Int. Conf. on Acoustics, Speech and Signal Processing, 2009, pp. 2149–2152

[17] Gao, X., Zhang, X., Sun, Z., *et al.*: 'On multilinear-based approaches of blind receiver for polarization sensitive uniform square array'. Int. Conf. on Wireless Networks and Information Systems, 2009, pp. 338–342

[18] Chen, L., Aminaei, A., Falcke, H., *et al.*: 'Optimized estimation of the direction of arrival with single tripole antenna'. Loughborough Antennas and Propagation Conf., 2010, pp. 93–96

[19] Gong, X.: 'Source localization via trilinear decomposition of cross covariance tensor with vector-sensor arrays'. Int. Conf. on Fuzzy Systems and Knowledge Discovery, 2010, pp. 2119–2123

[20] Gong, X.-F., Liu, Z.-W., Xu, Y.-G.: 'Direction finding via biquaternion matrix diagonalization with vector-sensors', *Signal Process.*, 2012, **91**, pp. 821–831

[21] He, J., Ahmad, M.O., Swamy, M.N.S.: 'Extended-aperture angle-range estimation of multiple Fresnel-region sources with a linear tripole array using cumulants', *Signal Process.*, 2012, **92**, pp. 939–953
[22] Yuan, X.: 'Estimating the DOA and the polarization of a polynomial-phase signal using a single polarized vector-sensor', *IEEE Trans. Signal Process.*, 2012, **60**, (3), pp. 1270–1282
[23] Yuan, X., Wong, K.T., Xu, Z*., et al.*: 'Various triad compositions of collocated dipoles/loops, for direction finding & polarization estimation', *IEEE Sens. J.*, 2012, **12**, (6), pp. 1763–1771
[24] Duzel, T., Akleman, F.: 'Direction of arrival estimation in the vicinity of source using vector sensor'. IEEE Int. Symp. on Phased Array Systems & Technology, 2013, pp. 541–546
[25] Jin, H., Wei-Wei, J., Wei-ping, L*., et al.*: 'Angle-polarization estimation & tracking for coherent signals using a linear tripole array'. Aerospace Shanghai, January 2015
[26] Gallee, F., Chainon, S., Lattard, H*., et al.*: 'Development of an isotropic sensor 2–6 GHz'. European Microwave Conf., 2007, pp. 91–93
[27] Compton, R.T.Jr.: 'The tripole antenna: an adaptive array with full polarization flexibility', *IEEE Trans. Antennas Propag.*, 1981, **29**, (6), pp. 944–952
[28] See, C.-M.S., Nehorai, A.: 'Source localization with distributed electromagnetic component sensor array processing'. Int. Symp. on Signal Processing & Its Applications, 2003, vol. **1**, pp. 177–180
[29] Au-Yeung, C.K., Wong, K.T.: 'CRB: sinusoid-sources' estimation using collocated dipoles/loops', *IEEE Trans. Aerosp. Electron. Syst.*, 2009, **45**, (1), pp. 94–109
[30] Xu, Z., Yuan, X.: 'Cramér-Rao bounds of angle-of-arrival and polarisation estimation for various triads', *IET Microw. Antennas Propag.*, 2012, **6**, (15), pp. 1651–1664
[31] Wong, K.T., Wu, Y.I., Hsu, Y.-S*., et al.*: 'A lower bound of DOA-estimates by an array randomly subject to sensor-breakdown', *IEEE Sens. J.*, 2012, **12**, (5), pp. 911–913
[32] Song, Y., Wong, K.T.: 'A lower bound of direction-of-arrival estimation for an acoustic vector sensor subject to sensor breakdown', *IEEE Trans. Aerosp. Electron. Syst.*, 2012, **48**, (4), pp. 3703–3708
[33] Castanie, F.: '*Digital spectral analysis: parametric, non-parametric and advanced methods*' (John Wiley and Sons, New York, NY, 2011)